JOURNAL OF GEOPHYSICAL RESEARCH, VOL. 103, NO. B7, PAGES 15,037–15,050, JULY 10, 1998

Intrinsic and scattering seismic wave attenuation in the Canary Islands

José Antonio Canas,[1] Arantza Ugalde,[2,3] Luis G. Pujades,[2]
Juan Carlos Carracedo,[4] Vicente Soler,[4] and María José Blanco[5]

Abstract. The Canary Islands volcanic complex is studied in terms of coda wave attenuation. A multiple lapse time window method, based on the hypothesis of multiple isotropic scattering with uniform distribution of scatterers, is applied to the available seismic data in order to obtain the intrinsic absorption (Q_i^{-1}) and the scattering attenuation (Q_s^{-1}) in the Canarian lithosphere. The analysis is performed for two hypocentral distance ranges: from 0 to 80 km and from 0 to 140 km. Results show that in both cases and for all the studied frequency bands (1-2, 2-4, 6-8 and 8-10 Hz) intrinsic absorption dominates. The low albedos found in the region indicate the low degree of heterogeneity in the Canarian lithosphere at the scale length of the studied frequencies. On the other hand the coda attenuation (Q_c^{-1}) calculated on the basis of the single-scattering theory gives values near Q_i^{-1} for low frequencies and near the total attenuation (Q_t^{-1}) for high frequencies. The degree of frequency dependence of the attenuation parameters is strong in all cases. A correlation of the observed attenuation parameters with the geological evidence for a hotspot-type archipelago and with other geophysical studies is suggested.

1. Introduction

The Canary Islands are an intraplate volcanic archipelago situated between 27.4° and 29.3°N and 13.2° and 18.9°W on a slow moving oceanic plate (the Atlantic). They consist of seven main islands located close to the west continental African edge. This passive border is expected to have a stable behavior, but the passive African margin is an atypical case of passive edges since it possesses strong tectonic and magmatic processes as the existence of the Canary Islands, Madeira, and Cape Verde demonstrates. A significant research on the archipelago has been performed during the last 25 years. A number of geological and geophysical studies have been carried out [*Carracedo*, 1984; *Mézcua et al.*, 1991; *Canales*, 1997]. However, because of the important geodynamical complexity of the region, different theories have been proposed for the genesis of the islands, and a unique model has not been generally accepted, although a hotspot origin hypothesis is gaining wide acceptance [*Hoernle and Schmincke*, 1993; *Carracedo et al.*, 1997]. The geophysical studies carried out in this region were directed toward obtaining seismic reflection data, gravity, and magnetics [*Watts*, 1994; *Dañobeitia et al.*, 1994; *Geisslinger et al.*, 1996]. *Canas et al.* [1995] used the first high-quality seismic recordings from earthquakes in the archipelago to determine the attenuation of seismic energy using coda waves.

Coda waves constitute a powerful tool for the calculation of seismic wave attenuation in the Earth's lithosphere. Total anelastic attenuation of a body wave can be characterized by the inverse quality factor Q_t^{-1} defined as the fraction of energy lost during a wave cycle. Two effects contribute to the observed total attenuation as expressed by the equation $Q_t^{-1} = Q_i^{-1} + Q_s^{-1}$ [*Dainty*, 1981]. Q_i^{-1} represents the intrinsic absorption caused by the conversion of seismic energy into heat, and Q_s^{-1} is the scattering attenuation because of the redistribution of energy that occurs when seismic waves interact with the heterogeneities of the medium. Many theoretical studies have been developed to model the coda shape. *Aki and Chouet* [1975] proposed the single backscattering model under the assumption of weak scattering. The inverse quality factors obtained within this context have been called Q_c^{-1} or coda-Q^{-1}. *Canas et al.* [1995] estimated the values of Q_c^{-1} for the Canary Islands by means of a modified version [*Pujades et al.*, 1990] of the method of *Herrmann* [1980] based on the single scattering pioneer work of *Aki* [1969]. They mapped iso-Q_0 lines (Q_c for the frequency 1 Hz) for

[1]Instituto Geográfico Nacional, Madrid, Spain.
[2]Universitat Politècnica de Catalunya, Enginyeria del Terreny i Cartogràfica, Barcelona, Spain.
[3]Now at Observatori de l'Ebre, Roquetes, Spain.
[4]Estación Volcanológica de Canarias, La Laguna, Spain.
[5]Instituto Geográfico Nacional, Santa Cruz de Tenerife, Spain.

Paper number 98JB00769.
0148-0227/98/98JB-00769$09.00

the studied region. However, multiple scattering models were necessary to determine the contribution of the scattering loss Q_s^{-1} to total attenuation. A multiple scattering model, under the assumptions of isotropic scattering and uniform distribution of scatterers, was considered by *Wu* [1985], who modeled the spatial distribution of the seismic energy integrated over infinite time. Under the same hypothesis of *Wu* [1985], *Hoshiba* [1991] modeled the spatial and temporal distribution of the multiscattered seismic wave energy using a Monte-Carlo numerical simulation [*Abubakirov and Gusev*, 1990]. *Zeng et al.* [1991] found the numerical solution of the same problem from an integral equation.

In the present study the multiple lapse time window analysis (MLTWA) of *Hoshiba et al.* [1991], which gives the temporal change of seismic energy while the wave is propagating, will be applied to seismic data from the Canary Islands. The following assumptions are made: scattering is multiple and isotropic; the distribution of scatterers is uniform; and the coda is only composed of S to S scattered waves. Two attenuation parameters are calculated [*Wu*, 1985]: the seismic albedo (B_0), defined as the dimensionless ratio of the scattering loss to total attenuation, and the inverse of the extinction length L_e^{-1} that is the inverse of the distance (in kilometers) over which the primary S wave energy is decreased by e^{-1}. The multiple lapse time window method allows one to estimate B_0 and L_e^{-1} by comparing the energy density predicted by the multiple isotropic scattering theory in space and time with the observations. The inverse quality factors Q_t^{-1}, Q_s^{-1}, and Q_i^{-1} are then calculated through the expressions $Q_t^{-1} = L_e^{-1}\,\frac{v}{\omega}$, $Q_s^{-1} = B_0\,Q_t^{-1}$, and $Q_i^{-1} = (1 - B_0)\,Q_t^{-1}$ [*Hoshiba et al.*, 1991]. The shear wave velocity v in this region is assumed to be 4 km s^{-1}.

The MLTWA has been widely applied to different regions in the world: *Fehler et al.* [1992] in the Kanto-Tokai region (Japan), *Mayeda et al.* [1992] in Hawaii, Long Valley, and central California, *Hoshiba* [1993] in Japan, *Jin et al.* [1994] in southern California, *Akinci et al.* [1995] in southern Spain and western Anatolia (Turkey), and *Pujades et al.* [1997] in the southeastern Iberian peninsula. In the present study the Canary Islands will be studied in terms of the anelastic attenuation by means of the MLTWA. Estimates of total attenuation Q_t^{-1} will be compared with the coda-Q^{-1} values obtained in a previous work by *Canas et al.* [1995]. We will suggest a correlation of the observed contrasting geological and structural features of the islands with the high observed seismic attenuation in the region. This paper is an attempt to establish some clear constraints that may help to throw light on the complex genesis and development of the Canarian Archipelago.

2. Geological Framework

It is believed that the Canary Islands are a hotspot-induced active volcanic chain located in close vicinity to the passive African continental margin and aligned in the direction of the plate motion (Figure 1). The seven islands of the archipelago rest on Jurassic age oceanic crust [*Hayes and Rabinowitz*, 1975] and were formed during the Neogene through multiple volcanic episodes [*Watkins*, 1974; *Carracedo*, 1979]. The origin and evolution of the Canarian Archipelago are far from being well explained and modeled because of several circum-

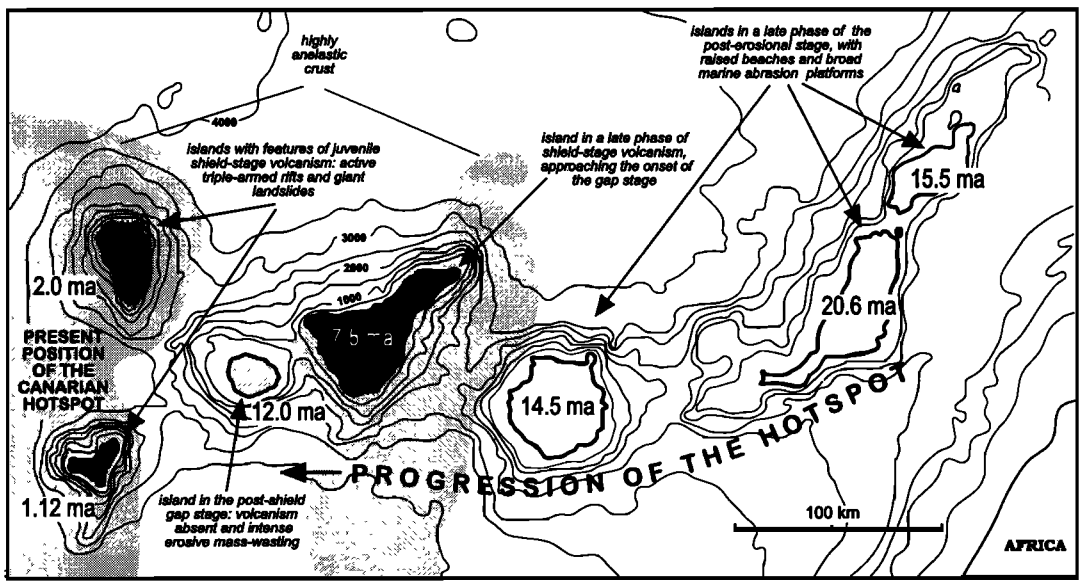

Figure 1. Present stage of the evolution of the Canary Islands. The postulated progression and present position of the Canarian hotspot as well as the oldest published K-Ar ages of the subaerial volcanics of the Canary Islands are shown. As defined in the Hawaiian Islands, the Canaries can be separated into three distinct groups: islands in the shield stage, in the gap stage, and in the post-erosional stage of development. The shaded areas indicate zones of highly anelastic lithosphere [*Canas et al.*, 1995].

stances such as the complexities of the geology of the Canaries, in particular, to the east of the archipelago.

Concrete evidence for the relative roles of regional tectonics and mantle plumes in the genesis of the islands may come from large-scale seismological and structural studies of the deep structure of the surrounding oceanic lithosphere and from constraints provided by geochemical and isotopic features of the magmas involved. The analysis of the existing geological information from the islands themselves, especially the timing of eruptive activity and their morphological and structural features, may help to establish some clear constraints that may narrow down the range of acceptable models for the genesis and development of the archipelago.

Geological and geochronological work carried out in the western Canaries has revealed the presence of contrasting development patterns and structural features (see Figure 1) with those of the eastern islands [*Carracedo*, 1994; *Carracedo and Day*, 1995; *Carracedo et al.*, 1997]. These contrasting features may be explained by the complex geological framework in which the islands emerged, which is characterized by two main circumstances: (1) the activity of a relatively slow motion, long-lived hotspot [*Holik et al.*, 1991] and (2) the lateral variations in the nature and rigidity of the lithosphere when progressing from the continent toward the oceanic (westernmost) edge of the volcanic chain [*McFarlane and Ridley*, 1968; *Bosshard and McFarlane*, 1970; *Banda et al.*, 1981].

The effects of tensional stresses on the archipelago, associated with the South Atlas Alpine orogeny, have been postulated as one of the main factors generating the volcanism and volcanic features of the Canaries [*Anguita and Hernán*, 1975, 1986].

A comparison of the Canarian Archipelago with the prototypical hotspot-related island group, the Hawaiian Archipelago, reveals that the differences between the two are not as great as had previously been supposed on the basis of older data. Quaternary igneous activity in the Canaries is concentrated at the western end of the archipelago, close to the present-day location of the inferred hotspot (Figure 1). Individual islands in both archipelagos are characterized by initial rapid growth (the shield-building stages of activity) followed by a period of quiescence and deep erosion (erosion gap) which in turn is followed by a posterosional stage of activity. This stage of activity is more intense in the Canary Islands than in the Hawaiian Islands, perhaps because of the much lower plate velocity which means that the islands remain in the vicinity of the underlying mantle anomaly.

A comparison of the structure and structural evolution of the Canary Islands with those of other oceanic islands, Hawaii, Réunion, etc., reveals many similarities, such as the development of triple "Mercedes Star" rift zones [*Carracedo*, 1994] and the occurrence of giant lateral collapses on the flanks of these rift zones [*Carracedo*, 1994, 1996; *Watts and Masson*, 1995; *Carracedo et al.*, 1997]. The absence of these features in the posterosional islands may, in part, be a result of their greater age and deeper erosion, which has removed much of the evidence of their early volcanic architecture.

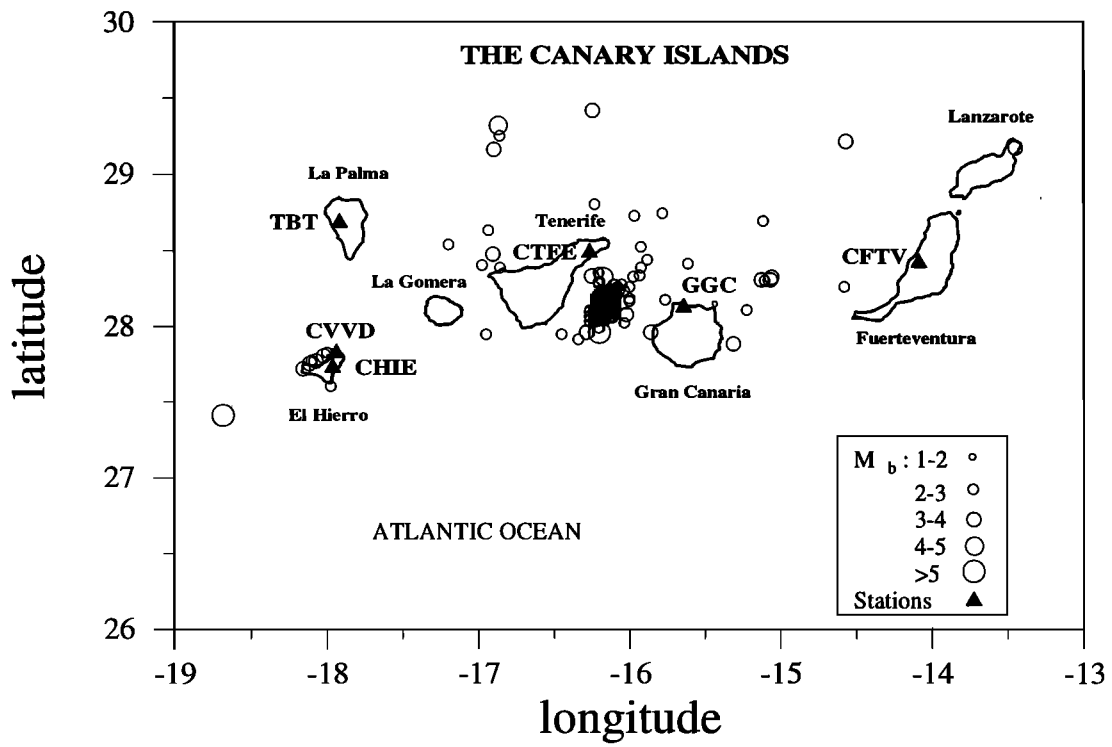

Figure 2. Geographical location of the Canary Islands. The name of the seven main islands and the codes of the six seismic stations are alsc shown. The circles represent the location of the earthquakes used in this study.

Table 1. Geographical Location, Recording Component, Characteristic Period, and Recording System of the Stations of the Canarian Seismic Network

Station	Code	Latitude	Longitude	h, m	Component	T_0, s	Recording System
Aguarijo (El Hierro)	CVVD	27°49'15"N	17°56'10"W	450	Z	1	ink sprengnether 60 mm s^{-1}
Betancuria (Fuerteventura)	CFTV	28°24'50"N	14°05'00"W	540	Z	1	thermal kinemetrics 60 mm s^{-1}
Guía (Gran Canaria)	GGC	28°07'11"N	15°38'12"W	560	Z	1	thermal kinemetrics 60 mm s^{-1}
Las Mesas (Tenerife)	CTFE	28°28'46"N	16°15'44"W	270	Z,N,E	0.85	ink volk 120 mm s^{-1}
					Z	1	ink volk 120 mm s^{-1}
Las Playas (El Hierro)	CHIE	27°43'37"N	17°57'39"W	170	Z	1	thermal kinemetrics 60 mm s^{-1}
Taburiente (La Palma)	TBT	28°40'46"N	17°54'52"W	180	Z	1	thermal kinemetrics 60 mm s^{-1}

Only analog data were available

3. Seismic Data

Seismic activity in the Canary Islands is moderate with earthquake magnitudes usually <5. Volcanic and tectonic earthquakes occur in this area with the NE-SW reverse fault between the islands of Tenerife and Gran Canaria [*Mézcua et al.*, 1990] being the source of almost all the tectonic seismic activity of the region since 1989.

The Canarian seismic network that belongs to the Red Sismológica Nacional of the Instituto Geográfico Nacional is composed of six short period seismographic stations that are distributed along the entire archipelago (Figure 2). In Table 1 the geographical location, recording seismic component, characteristic period, and recording system of each station used in this study are shown. From the seismometer characteristics in Table 1 it is seen that only analog short period data were available in this study, so it was necessary to manually digitize the data prior to analysis. A total of 87 seismograms with epicentral distances <216 km, magnitudes ranging from 2 to 4, and focal depths <54 km were analyzed (Figure 2).

4. Method of Analysis

The multiple lapse time window method [*Hoshiba et al.*, 1991] consists of comparing the predicted seismic energy in some lapse time windows measured from the S wave onset as a function of hypocentral distance, with the observations, to obtain the values of the seismic albedo B_0 and the inverse of the extinction length L_e^{-1} in a specified frequency band. The observed seismic energies as a function of hypocentral distance are calculated following *Hoshiba* [1993]. First, the mean square amplitudes of the bandpass-filtered waveforms as a function of lapse time t are calculated for each seismogram, obtaining $A_{\text{obs}}(f|r,t)$. Then, by integrating this function over three consecutive time windows: 0-15, 15-30, and 30-45 s measured from the S wave onset the energies in the early, middle, and late coda represented by the function $e_{n\ \text{obs}}(f|r)$, $(n = 1,2,3)$ are calculated. A correction for different earthquake sources and site amplification factors is performed using the coda normalization technique [*Aki*, 1980] to obtain

$$E_{n\ \text{obs}}(f|r) = \frac{e_{n\ \text{obs}}(f|r)}{A_{\text{obs}}(f|r,t_{\text{ref}})} \qquad n = 1,2,3 \quad (1)$$

where $E_{n\ \text{obs}}(f|r)$ represent the normalized observed seismic energies for the center frequency f and the nth time window. The parameter t_{ref} is a fixed reference lapse time that satisfies the condition $t_{\text{ref}} \geq \frac{2r}{v}$ for all r. A correction for the geometrical spreading effect is made by multiplying $E_{n\ \text{obs}}(f|r)$ by the factor $4\pi r^2$, which only applies to body waves in a uniform medium.

The model curves of the energy density at a given lapse time and hypocentral distance, under the assumptions of multiple isotropic scattering and uniform distribution of scatterers, are calculated by means of the following equation [*Zeng et al.*, 1991]:

$$E(\vec{r},t) = E_0\left(t - \frac{|\vec{r}-\vec{r}_0|}{v}\right)\frac{e^{-L_e^{-1}|\vec{r}-\vec{r}_0|}}{4\pi|\vec{r}-\vec{r}_0|^2} + \int_V g\,E\left(\vec{r}_1, t - \frac{|\vec{r}_1-\vec{r}|}{v}\right)\frac{e^{-L_e^{-1}|\vec{r}_1-\vec{r}|}}{4\pi|\vec{r}_1-\vec{r}|^2}\,dV_1 \quad (2)$$

where $E(\vec{r},t)$ is the seismic energy density per unit volume at position $\vec{r}$ and time t for a point source at $t = 0$ located at $\vec{r}_0$. The first term on the right-hand side of (2) represents the direct wave energy, and the second term is the contribution of scattered energy of all orders. The parameter v is the S wave velocity and $g = L_e^{-1}\,B_0$ is the scattering coefficient. A numerical solution of (2) for various combinations of L_e^{-1} and B_0 can be obtained by using a hybrid method that consists of combining analytical solutions for single scattering with a numerical solution based on the two-dimensional fast Fourier transform for multiple scattering [*Sato*, 1994]. Therefore the theoretical function $E(r,t)$ that represents the

energy received at hypocentral distance r and time t is obtained. This function is numerically integrated over the three considered consecutive time windows from the S wave onset and then normalized and corrected for the geometrical spreading effect following the same steps described for the observations.

The best fit model parameters are obtained by calculating the minimum residual between the predicted and the observed data by a multiple least squares regression. The ratio of the residual over the minimum residual for each parameter pair (L_e^{-1},B_0) is plotted, and the uncertainties associated with the parameters are calculated using F distribution tests.

5. Results

The instrument characteristics and the manual data digitizing process limited the number of frequency bands to be studied. The following frequencies will be analyzed: 1-2, 2-4, 4-6, 6-8, and 8-10 Hz. From the bandpass-filtered data the function $A_{\rm obs}(f|r,t)$ was calculated by averaging the squared amplitudes in a time window of $t \pm 2$ s for the frequency band centered at 1.5 Hz and $t \pm 1$ s for the other frequency bands. An example of a function $A_{\rm obs}(f|r,t)$ for an actual seismogram used is shown in Figure 3.

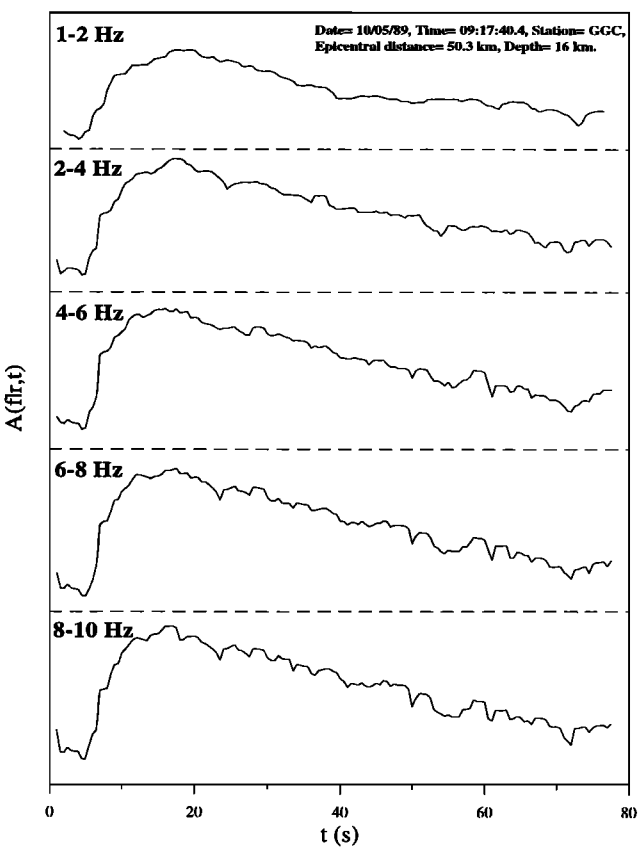

Figure 3. Mean square amplitudes as a function of time for an actual bandpass-filtered seismogram. It corresponds to the station GGC and the date and origin time of the earthquake are May 10, 1989, and 0917:40.4 UT. The magnitude of the event was 2.9, and the depth was 16 km.

The estimation of L_e^{-1} and B_0 by means of the MLTWA was performed for two hypocentral distance ranges: 0-80 and 0-140 km. For each distance range the normalized observed energies were calculated by means of (1), choosing $t_{\rm ref}$ as a 5 s length time window centered at 45 and 70 s for the 0-80 and 0-140 km distance ranges, respectively. It is worth mentioning that only amplitudes with a signal to noise ratio >2 were considered for all the calculations. Some seismograms with hypocentral distances from 140 to 216 km were also available, but they had to be discarded because the fit between the theoretical and observed data was poor because of the few points at short distances for lapse times >100 s. The coda normalization technique, represented by (1) in the present study, makes a correction for the source shape, not for the radiation pattern function. Therefore a smoothing process was applied to the observed data by averaging the energy in a moving window of 5 km length overlapping 2.5 km. This smoothing is equivalent to the case of isotropic source radiation [*Hoshiba*, 1993].

The best fit model parameters L_e^{-1} and B_0 were calculated by means of a multiple least squares regression between the smoothed observed data and the theoretical curves, where the synthetics were obtained by solving (2) numerically. In Figures 4 and 5 the theoretical curves best fitting the observed data are plotted for the five studied frequency bands and for the two hypocentral distance ranges. The data represented in Figures 4 and 5 are the observations, without any smoothing, and the continuous lines represent the best fit using the smoothed data. Two examples of the ratios residual/minimum residual are plotted in Figure 6. The unshaded zones correspond to the confidence areas calculated by the application of the F distribution test at the 90% confidence level. Table 2 contains the estimated attenuation parameters L_e^{-1}, B_0, Q_i^{-1}, Q_s^{-1} and Q_t^{-1} with their respective associated errors. These errors are not symetric because of the assymetry of the confidence areas (Figure 6).

6. Discussion

6.1. Coda-Q^{-1}

The decay rate of the coda amplitudes Q_c^{-1} can be estimated by applying the following equation based on the single scattering approximation [*Aki and Chouet*, 1975]:

$$\ln[t^2\, A_{\rm obs}(f|r,t)] = c - Q_c^{-1}\, 2\pi f t \qquad (3)$$

where c is a constant and $A_{obs}(f|r,t)$ represents the mean square amplitudes of the bandpass-filtered waveforms as a function of hypocentral distance r and lapse time t measured from the origin time of the earthquake. Empirically, (3) holds for $t > 2\ t_S$, where t_S is the S wave travel time [*Rautian and Khalturin*, 1978].

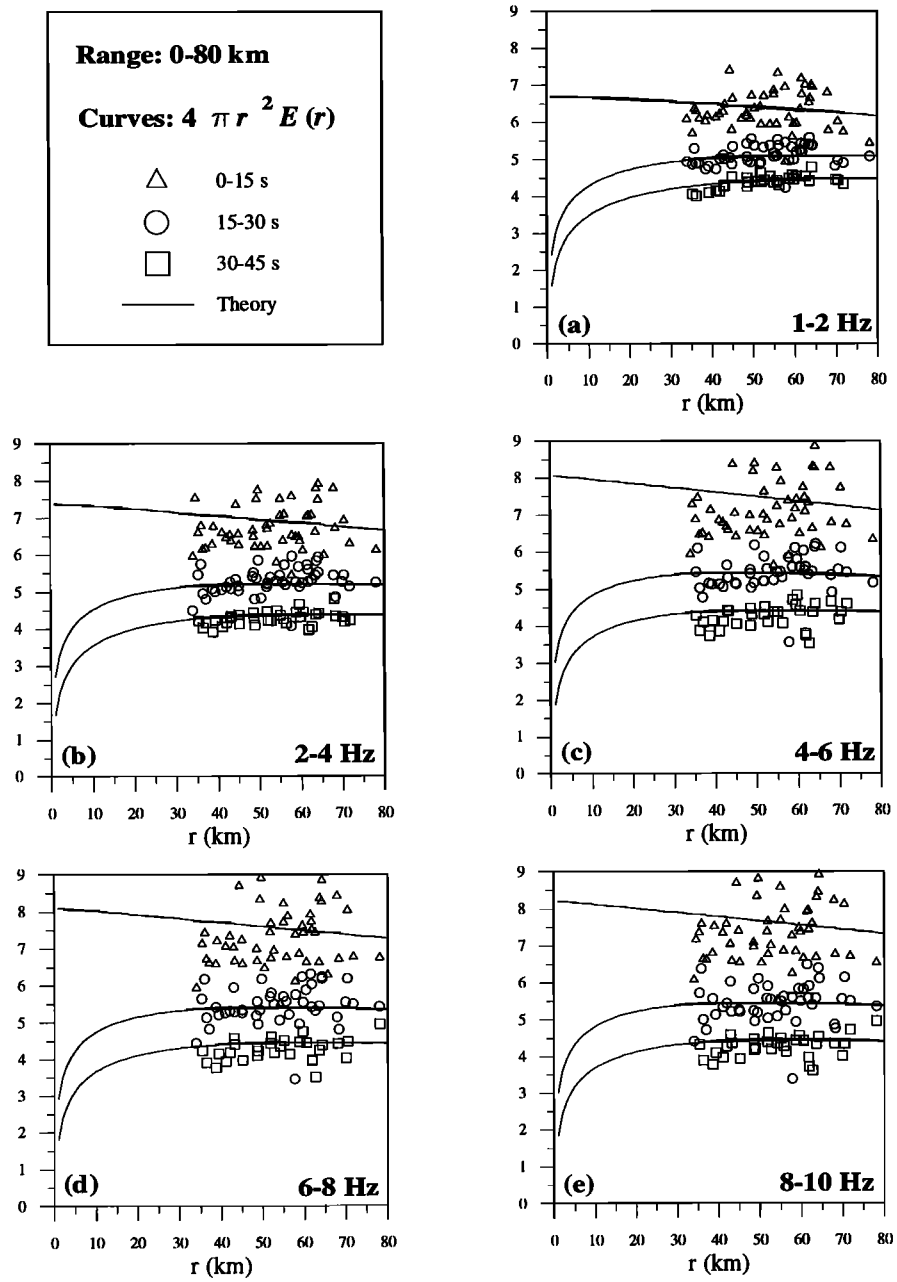

Figure 4. The observed integrated seismic energies for the 0-15 s lapse time window (triangles), 15-30 s (circles), and 30-45 s (squares) are plotted. The continuous lines represent the synthetic energy best fitting the observed data for (a) 1-2, (b) 2-4, (c) 4-6, (d) 6-8, and (e) for 8-10 Hz frequency bands. These results are those obtained for the 0-80 km hypocentral distance ranges.

A time window of $2\frac{r}{v}$ s to $2\frac{r}{v} + 40$ s from the origin time of the earthquake was adopted to perform a least squares regression applied to (3) for each frequency band. The resulting Q_c^{-1} estimates are plotted in Figure 7, where a dot represents Q_c^{-1} from a single seismogram. Earthquakes with hypocentral distances from 0 to 80 km and from 0 to 140 km were used to calculate Q_c^{-1}. Results are shown in Table 2. However, some theoretical studies [*Frankel and Wennerberg*, 1987; *Hoshiba*, 1991] point out that Q_c^{-1} is not a good approximation of Q_i^{-1} when multiple scattering is significant (except for the case $gvt << 1$ and $Q_s^{-1} << Q_i^{-1}$, where g is the scattering coefficient, v is the S wave velocity, and t is the lapse time). The expected values of Q_c^{-1} can be calculated by using the expression [*Hoshiba*, 1991]

$$\bar{Q}_c^{-1} = Q_s^{-1}\left[1 - \frac{C_2 + 2C_3(gvt) + 3C_4(gvt)^2 + \ldots}{1 + C_2(gvt) + C_3(gvt)^2 + \ldots}\right] + Q_i^{-1} \quad (4)$$

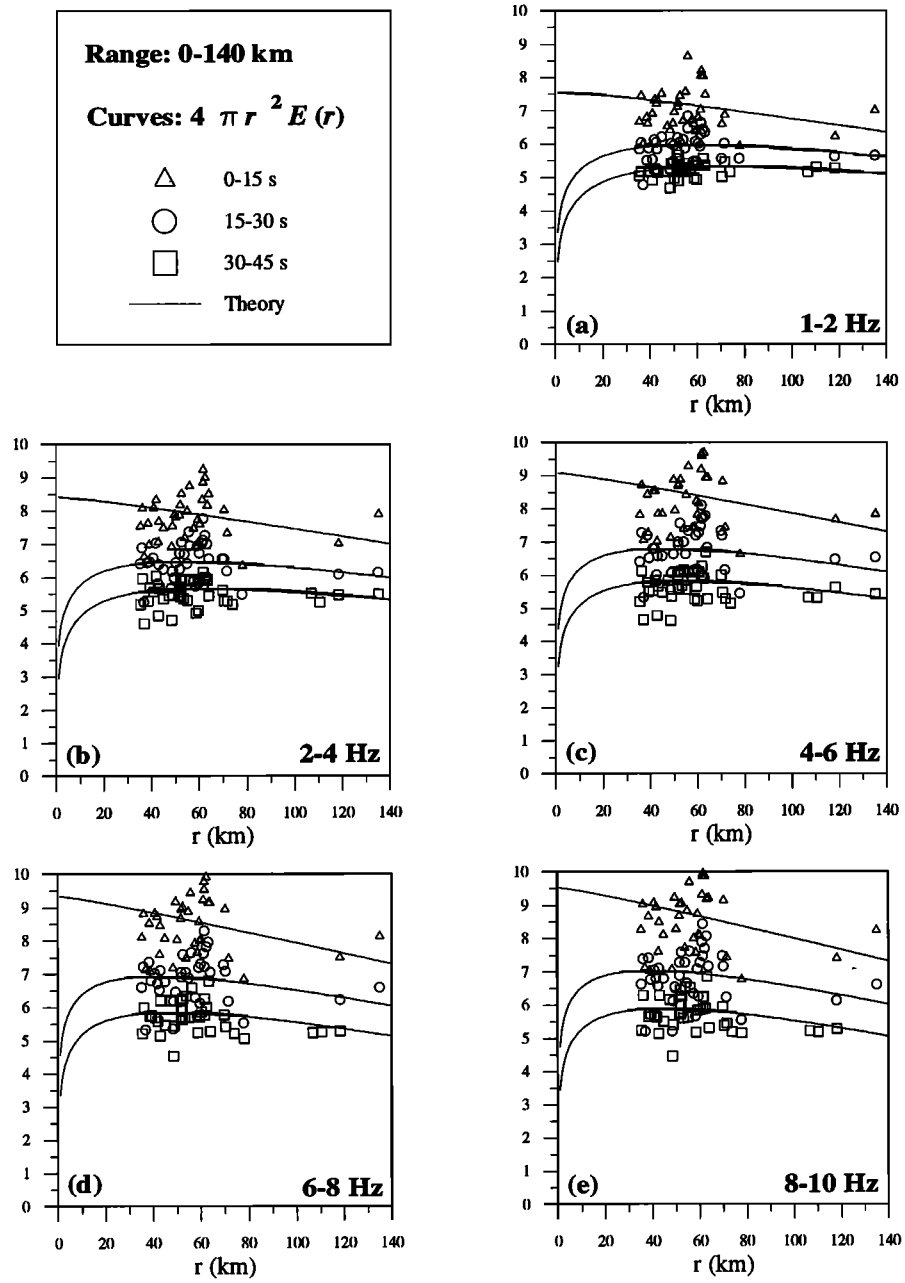

Figure 5. The same as Figure 3 but for the 0-140 km hypocentral distance range.

where C_n are constants listed in Table 1 of *Hoshiba* [1991].

Table 2 shows the values for $\bar{Q}_c^{-1}$ predicted by means of (4) for $t = 40$ s and for the two hypocentral distance ranges. Given the confidence bounds, we conclude that $\bar{Q}_c^{-1}$ is close to Q_c^{-1} and that Q_c^{-1} is similar to Q_i^{-1} for this region.

6.2. Frequency Dependence

Fitting the values of Q_i^{-1}, Q_s^{-1}, and Q_t^{-1} shown in Table 2 by means of a frequency law $Q^{-1}(f) = Q_0^{-1} f^{-\nu}$ we obtain

$$Q_i^{-1} = (9.1 \pm 1.2)\text{x}10^{-3}\, \text{f}^{(-0.70\pm0.08)}$$
$$Q_s^{-1} = (7.9 \pm 1.0)\text{x}10^{-3}\, \text{f}^{(-1.69\pm0.08)}$$
$$Q_t^{-1} = (14.7 \pm 1.1)\text{x}10^{-3}\, \text{f}^{(-0.88\pm0.05)}$$
$$Q_c^{-1} = (9.7 \pm 1.0)\text{x}10^{-3}\, \text{f}^{(-0.58\pm0.06)}$$

for the 0-80 km hypocentral distance range and

$$Q_i^{-1} = (8.3 \pm 0.1)\text{x}10^{-3}\, \text{f}^{(-0.58\pm0.01)}$$
$$Q_s^{-1} = (6.6 \pm 1.1)\text{x}10^{-3}\, \text{f}^{(-1.07\pm0.11)}$$
$$Q_t^{-1} = (14.3 \pm 0.6)\text{x}10^{-3}\, \text{f}^{(-0.72\pm0.03)}$$
$$Q_c^{-1} = (9.6 \pm 0.9)\text{x}10^{-3}\, \text{f}^{(-0.57\pm0.06)}$$

for the 0-140 km hypocentral distance range.

Taking into account the error bars, no significant dif-

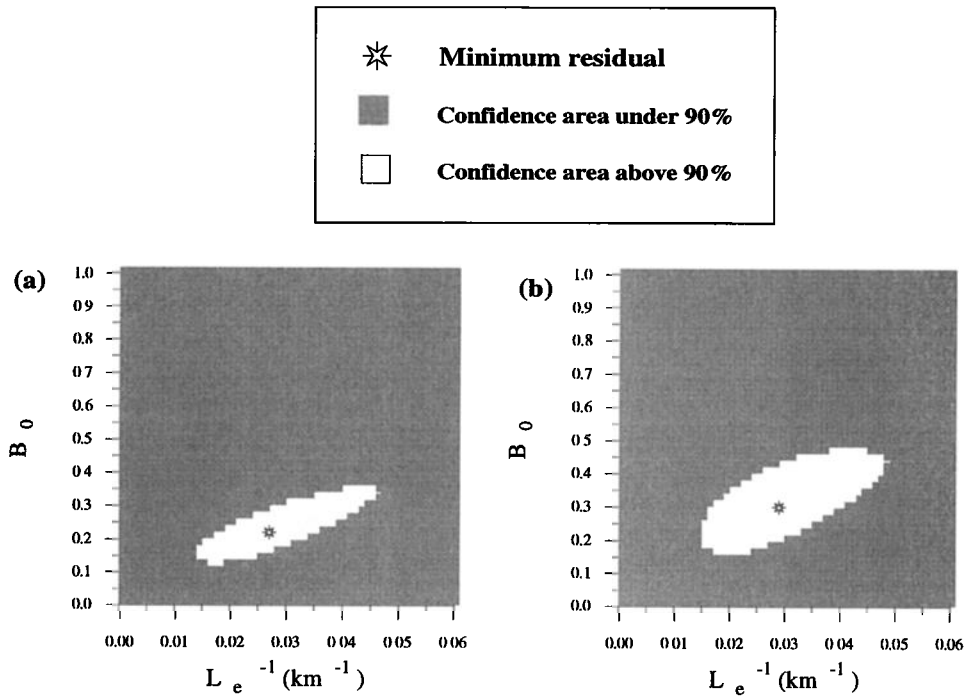

Figure 6. Residual plots and their associated error areas, calculated by means of the F test at the 90% level of confidence for the 2-4 Hz frequency band: (a) for the 0-80 km and (b) for the 0-140 km distance ranges. The unshaded area is the 90% confidence region.

Table 2. Attenuation parameters

Frequency, Hz	L_e^{-1}, km^{-1}	B_0	Q_i^{-1}x10^3	Q_s^{-1}x10^3	Q_t^{-1}x10^3	Q_c^{-1}x10^3	$\bar{Q}_c^{-1}$x10^3
			0-80 km				
1-2	0.024+0.024 -0.016	0.38+0.16 -0.14	6.3	3.9	10.2	7.2	5.1
2-4	0.027+0.021 -0.014	0.22+0.16 -0.12	4.5	1.3	5.8	5.5	4.0
4-6	0.031+0.021 -0.019	0.14+0.18 -0.10	3.4	0.6	4.0	4.2	3.0
6-8	0.027+0.028 -0.021	0.10+0.20 -0.08	2.2	0.3	2.5	3.2	2.2
8-10	0.029+0.024 -0.019	0.10+0.18 -0.08	1.8	0.2	2.0	2.5	1.7
			0-140 km				
1-2	0.027+0.017 -0.016	0.42+0.16 -0.18	6.6	4.8	11.4	7.2	4.7
2-4	0.029+0.021 -0.015	0.30+0.20 -0.16	4.3	1.8	6.1	5.3	3.5
4-6	0.034+0.023 -0.018	0.24+0.20 -0.16	3.3	1.0	4.3	4.2	2.6
6-8	0.039+0.026 -0.020	0.24+0.20 -0.16	2.7	0.9	3.6	3.2	2.1
8-10	0.042+0.028 -0.022	0.24+0.22 -0.16	2.3	0.7	3.0	2.5	1.7

Inverse extinction length, seismic albedo, intrinsic absorption, scattering attenuation, observed coda attenuation, and expected coda attenuation are shown. Two hypocentral distances have been considered: 0-80 and 0-140 km, and five center frequencies have been studied: 1.5, 3, 5, 7, and 9 Hz. The estimated values of the parameters have been obtained by the application of the multiple lapse time window analysis for isotropic scattering and uniform distribution of scatterers.

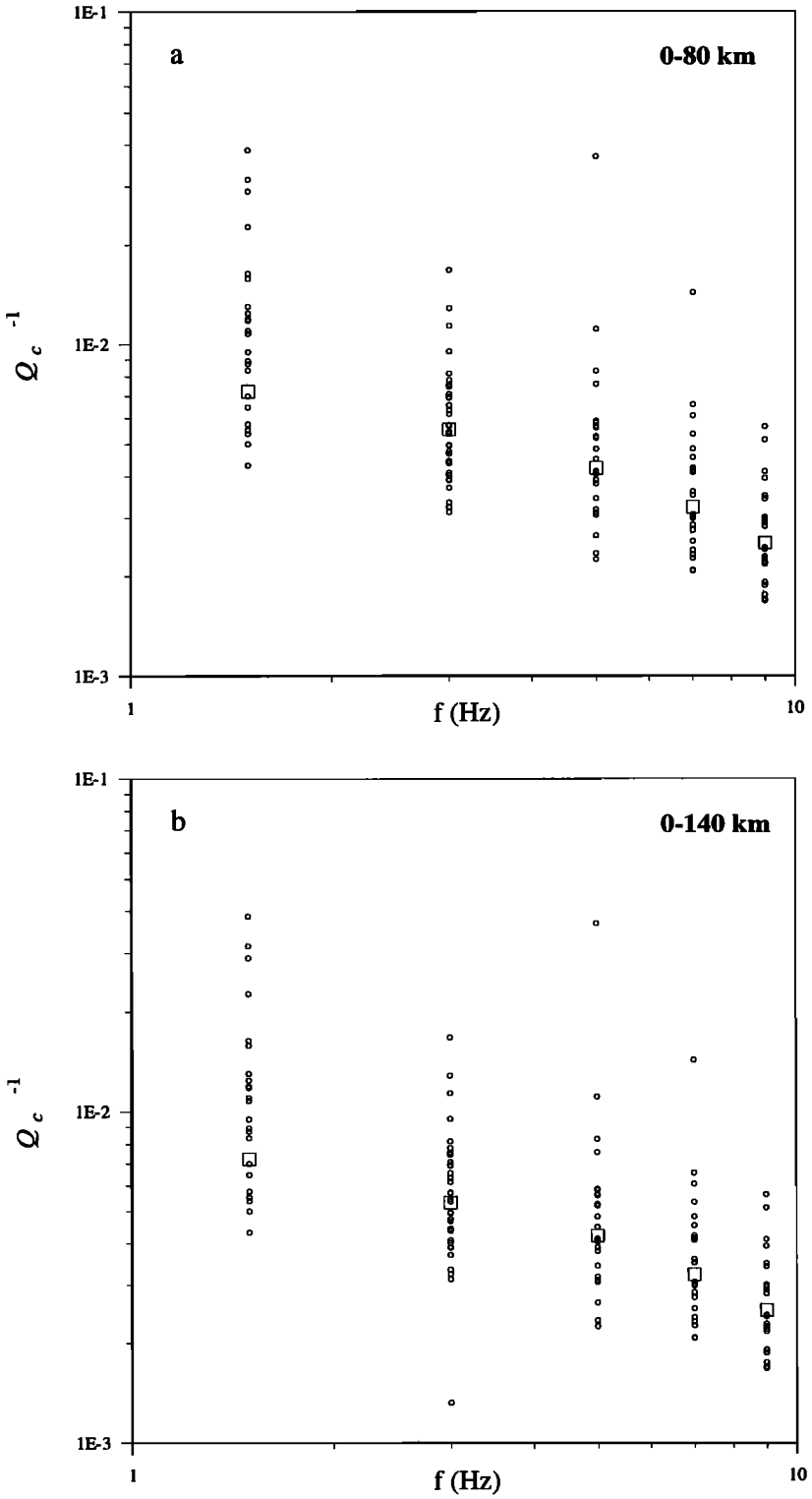

Figure 7. Coda Q^{-1} as a function of frequency for the 1.5, 3, 5, 7, and 9 Hz center frequencies. One circle represents the Q_c^{-1} value from a single seismogram and the squares are the mean of all the estimates for the studied frequencies for (a) 0-80 and (b) 0-140 km hypocentral distance ranges.

ferences are found between the frequency dependence for the 0-80 and 0-140 km hypocentral distance ranges for all the attenuation parameters, except for Q_s^{-1}, for which a strong frequency dependence is found from the 0-80 km data ($\nu = -1.69$) while a frequency dependent exponent near -1 is found from the 0-140 km data. A decrease of Q_s^{-1} faster than f^{-1} with increasing frequency implies that the medium may be characterized by a Gaussian rather than exponential autocorrelation function [*Wu*, 1985]. The strong frequency dependence

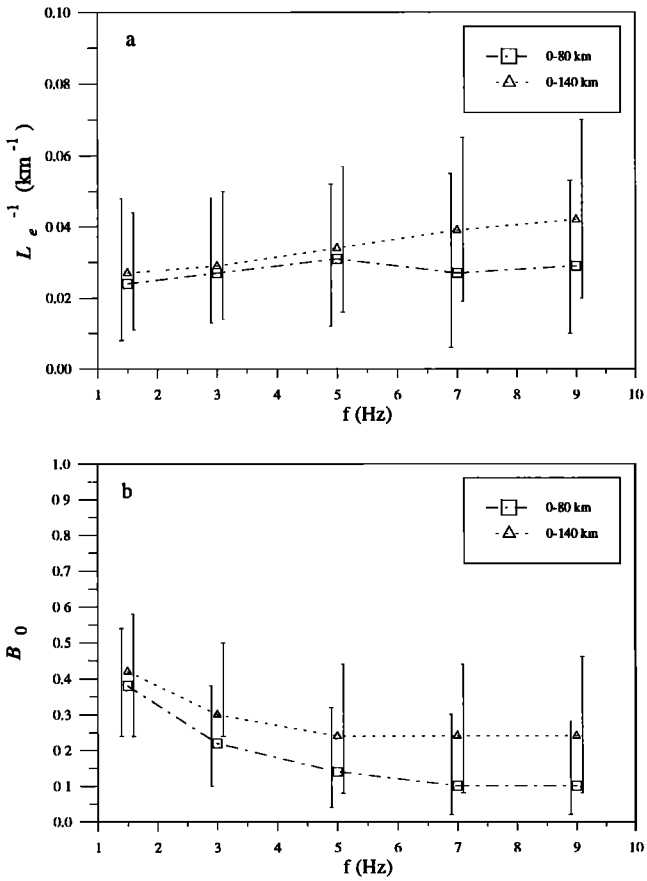

Figure 8. Estimates of the (a) inverse of the extinction length and (b) seismic albedo as a function of frequency for the 0-80 (squares) and 0-140 km (triangles) hypocentral distance ranges.

of Q_s^{-1} at short distances may be related to the size of heterogeneities [*Mayeda et al.*, 1992; *Jin et al.*, 1994; *Akinci et al.*, 1995], which would be comparable to the wavelength of the lowest analyzed frequencies.

The estimated values of L_e^{-1} and B_0 for the 0-80 and 0-140 km as a function of frequency are plotted in Figure 8. It can be seen that the inverse of the extinction length tends to increase with frequency, while the opposite is true for the seismic albedo. At a given frequency the estimated values are higher when considering the 0-140 km hypocentral distance range. Since B_0 is <0.5 for all frequencies and both hypocentral distance ranges the intrinsic absorption dominates over the scattering for the scale length of the studied frequencies in the region.

6.3. Comparison Among Q_i^{-1}, Q_s^{-1}, Q_t^{-1}, and Q_c^{-1}

The physical meaning of Q_c^{-1} within the context of the single scattering theory was that it represents the total attenuation. Nevertheless, some laboratory experiments [*Matsunami*, 1991] and theoretical studies [*Frankel and Wennerberg*, 1987; *Shang and Gao*, 1988; *Hoshiba*, 1991] demonstrated that Q_c^{-1} is not a measure of total attenuation but of the intrinsic absorption. Since many studies concerning the separation of the intrinsic absorption and scattering attenuation have been carried out in differents regions of the world a comparison between Q_c^{-1} and Q_i^{-1} can be performed. *Jin et al.* [1994] found that Q_c^{-1} is close to Q_i^{-1} for Japan and close to Q_t^{-1} for other regions (e.g., southern California), but in general, it is bounded between Q_i^{-1} and Q_t^{-1}. A comparative plot among the attenuation parameters in this study is presented in Figure 9, where Q_s^{-1} (triangles), Q_t^{-1} (squares), Q_i^{-1} (circles), and Q_c^{-1} (dashed line) are plotted as a function of Q_c^{-1}. For the 0-80 km distance range it can be seen that in the 1-2 Hz frequency band, Q_c^{-1} is close to Q_i^{-1}, but for high frequencies, Q_c^{-1} is close to Q_t^{-1}. For the 0-140 km hypocentral distance range, Q_c^{-1} is bounded between Q_i^{-1} and Q_t^{-1}. It can be seen (Table 2) that the estimates of L_e^{-1} and B_0 do not change significantly at short and long hypocentral distances and that the intrinsic absorption is the dominant attenuation effect for all frequencies.

6.4. Comparison With Other Attenuation Studies

The present paper is an extension of the studies of *Canas et al.* [1995] who obtained a detailed coda Q_0 map (Q_c for the frequency 1 Hz) for the Canarian Archipelago using the single scattering method described in *Pujades et al.* [1990]. They found Q_0 values between 60 and 300 with the lowest values located near the active fault between the islands of Tenerife and Gran Canaria. In the present study the single scattering theory [*Aki and Chouet*, 1975] has been applied using more frequency bands than were considered by *Canas et al.* [1995], and average values of Q_c have been obtained for the region in the ranges 0-80 and 0-140 km. From the frequency law obtained in this study for Q_c the inferred value of Q_0 is ~103 for both short and long hypocentral distances. We can say that our results for short hypocentral distances are in agreement with the lowest values obtained by *Canas et al.* [1995].

When comparing the multiple scattering results of the present work for the Canary Islands with the attenuation parameters estimated for other active areas, such as the southern Iberian peninsula [*Akinci et al.*, 1995], a big difference is seen. [*Akinci et al.*, 1995] obtained a strong scattering attenuation dominating over the intrinsic absorption for frequencies lower than 4 Hz and found similar Q_i^{-1} and Q_s^{-1} values for frequencies between 4 and 8 Hz. They also found a predominance of Q_s^{-1} at long hypocentral distances. However, results in the Canarian lithosphere show that a strong intrinsic absorption dominates over the scattering attenuation for all the studied frequencies and at short and long hypocentral distances. From these results it can be said that the attenuation processes are quiet different in the two regions (southern Spain and the Canary Islands).

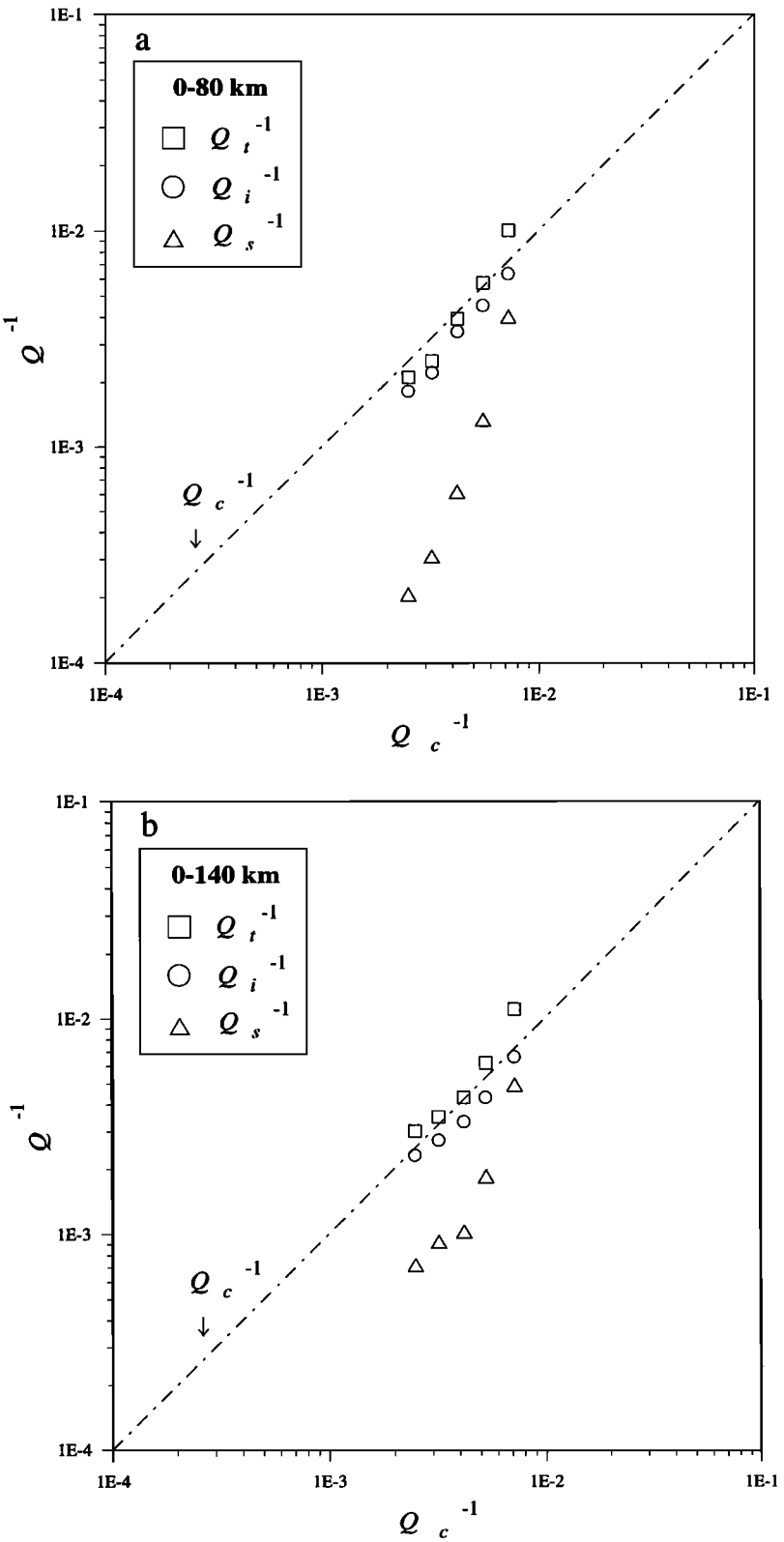

Figure 9. Plots of Q_t^{-1}, Q_i^{-1}, Q_s^{-1}, and Q_c^{-1} for each of the five frequency bands analyzed as a function of Q_c^{-1} for (a) 0-80 and (b) 0-140 km hypocentral distance ranges. Q_c^{-1} is between Q_i^{-1} and Q_t^{-1} for low frequencies, and it is close to Q_i^{-1} for high frequencies. Intrinsic absorption is found to be larger than scattering attenuation for all the studied frequencies.

6.5. Correlation With the Geological Features and Other Geophysical Results

The genesis of the Canary Islands has been explained by means of different theories, but on the basis of the geological information available the mantle plume model seems to explain many of the apparent inconsistencies pointed out in the development of the Canarian Archipelago [*Carracedo et al.*, 1998]. Figure 1 summarizes the evolutive stages of the Canaries: the islands of La Palma and El Hierro are in the early phases of the shield-stage volcanism, whereas the eastern islands (La Gomera, Fuerteventura, and Lanzarote) are in a late phase of posterosional stage. As Figure 1 shows, the first manifestation of the hotspot would have been located at the west of the island of Fuerteventura, and it would have moved through the western part of the Canarian chain.

The shaded areas in Figure 1 indicate the zones of high seismic attenuation estimated by *Canas et al.* [1995]. *Canas et al.* [1995] proposed that the low Q_0 values found in this region might indicate the presence of important lateral heterogeneities in the crust, magmatic sources under the islands, or a strong astenosphere (rejuvenated lithosphere) probably in relation with the passage of the hotspot.

Canales [1997] and *Canales and Dañobeitia* [1997] studied the structure of the lithospere underneath the Canarian Archipelago and obtained an average elastic thickness of 32-35 km for the Canarian lithosphere. On the basis of these studies, *Canales* [1997] defined the Canary Islands as a "weak hotspot" and concluded that the interaction between the mantle plume and the oceanic lithosphere may produce a change in the thermal structure of the lithosphere at depths >50 km. This interpretation does not require significant thermal rejuvenation of the lithosphere. Nevertheless, other geophysical studies [*Watts*, 1994] have suggested the hypothesis of a lithospheric thinning.

On the other hand, the moderate seismicity of the region, situated in the passive and oldest part of the Atlantic Ocean, does not correlate with the strong observed total attenuation. The age of the Canarian lithosphere has been estimated by means of the magnetic anomalies with the result that the Canary Islands are located between the isochrones S1 (~170-175 My [*Roest et al.*, 1992]) and M25 (~156 My [*Verhoef et al.*, 1991]). However, the low estimated Q values would be expected in areas located in young oceanic regions [*Canas and Mitchell*, 1981]. Moreover, similar results are obtained at short and long hypocentral distances with a dominant intrinsic absorption. This fact might be consistent with the idea of the presence of a strong astenosphere under the archipelago, as pointed out by *Canas et al.* [1995], because at long hypocentral distances the seismic waves sample a deeper portion of the medium.

7. Conclusions

The attenuation of seismic shear waves in the Canary Islands was studied using the coda wave multiple lapse time window analysis [*Hoshiba*, 1991], which assumes multiple isotropic scattering and a uniform distribution of scatterers. The following conclusions were obtained:

1. Total attenuation is strong and greater than expected for this oldest part of the Atlantic Ocean, where the seismic activity is very moderate. Moreover, the intrinsic absorption dominates over the scattering attenuation at short and long hypocentral distances.

2. The seismic albedo is lower than 0.5 for all the studied frequencies and hypocentral distance ranges. This result indicates a low degree of heterogeneity for the scale length of the analyzed frequencies in the region.

3. The low scattering attenuation found in the region appears to be strongly frequency dependent for short hypocentral distances. The decrease of Q_s^{-1} is faster than f^{-1} with increasing frequencies which may be consistent with a medium characterized by a Gaussian autocorrelation function. The strong frequency dependence could be related to the size of the heterogeneities, at least comparable to the wavelength of the lowest analyzed frequencies.

4. At short hypocentral distances, observed Q_c^{-1} has been found to be close to the intrinsic absorption at low frequencies and close to total attenuation at high frequencies. For long distances, observed Q_c^{-1} is bounded by Q_i^{-1} and Q_t^{-1}.

5. The coda Q values at a frequency 1 Hz (Q_0) in the present study are in agreement with the lowest Q_0 values obtained by *Canas et al.* [1995]. Large differences in the attenuation parameters are found between geothermal (the Canary Islands) and non geothermal (e.g., southern Iberian peninsula) areas.

6. The geological evidence relative to a hotspot-type island and the high degree of attenuation with a dominance of the intrinsic absorption over the scattering attenuation for all the studied frequency bands and hypocentral distance ranges favors the hypothesis that a strong astenosphere is present in the region. Nevertheless, there are other possibilities. *Canas et al.* [1995] found that the strong attenuation was practically the same for volumes with depths ~76 km or volumes with depths ~230 km and a similar conclusion can be inferred from this study. This result could indicate the presence of material in state of partial melting causing the strong observed intrinsic absorption at short hypocentral distances. Finally, the explanation of the high observed attenuation parameters in terms of both the presence of a rejuvenated lithosphere and a material in state of partial melting are compatible with the hypothesis of the Canarian hotspot.

7. The MLTWA has improved our knowledge of the attenuation parameters in this region. However,

it would be necessary to consider more realistic models where intrinsic absorption and scattering vary with depth and for crustal velocity structure that is not a uniform half space.

Acknowledgments. We thank R. B. Herrmann, A. Frankel, and the Associate Editor G. Sutton for their constructive comments on improving the manuscript. This paper has been partially financed by CICYT and DGICYT; projects MAR95-1916, AMB96-0996, and PB95-0777.

References

Abubakirov, I. R., and A. A. Gusev, Estimation of scattering properties of lithosphere of Kamchatka based on Monte-Carlo simulation of record envelope of a near earthquake, *Phys. Earth Planet. Inter., 64*, 52-67, 1990.

Aki, K., Analysis of the seismic coda of local earthquakes as scattered waves, *J. Geophys. Res., 74*, 615-631, 1969.

Aki, K., Attenuation of shear-waves in the lithosphere for frequencies from 0.05 to 25 Hz, *Phys. Earth Planet. Inter., 21*, 50-60, 1980.

Aki, K., and B. Chouet, Origin of coda waves: Source, attenuation, and scattering effects, *J. Geophys. Res., 80*, 3322-3342, 1975.

Akinci, A., E. del Pezzo, and J. M. Ibáñez, Separation of scattering and intrinsic attenuation in southern Spain and western Anatolia (Turkey), *Geophys. J. Int., 121*, 337-353, 1995.

Anguita, F., and F. Hernán, A propagating fracture model versus a hotspot origin for the Canary Islands, *Earth Planet. Sci. Lett., 27*, 11-19, 1975.

Anguita, F., and F. Hernán, Geochronology of some Canarian dike swarms: Contribution to the volcano-tectonic evolution of the Archipelago, *J. Volcanol. Geotherm. Res., 30*, 155-162, 1986.

Banda, F., J. J. Dañobeitia, E. Suriñach, and J. Ansorge, Features of crustal structure under the Canary Islands, *Earth Planet. Sci. Lett., 55*, 11-24, 1981.

Bosshard, E., and D. J. McFarlane, Crustal structure of the western Canary Islands from seismic refraction and gravity data, *J. Geophys. Res., 75*, 4901-4918, 1970.

Canales, J. P., Interacción litosfera oceánica-punto caliente: Aplicación al volcanismo intraplaca (Archipiélagos de Canarias y Sociedad) y dorsal mesoceánica (Galápagos), Ph. D. thesis, Univ. of Barcelona, Barcelona, Spain, 1997.

Canales, J. P., and J. J. Dañobeitia, The Canary Islands swell: A coherence analysis of bathymetry and gravity, *Geophys. J. Int., 132*, 479-488, 1998.

Canas, J. A., and B. J. Mitchell, Rayleigh wave attenuation and its variation across the Atlantic Ocean, *Geophys. J. R. Astron. Soc. 67*, 159-176, 1981.

Canas, J. A., L. G. Pujades, M. J. Blanco, V. Soler, and J. C. Carracedo, Coda-Q distribution in the Canary Islands, *Tectonophysics, 246*, 245-261, 1995.

Carracedo, J. C., Paleomagnetismo e Historia Volcánica de Tenerife, report, Aula de Cult., Tenerife, Spain, 1979.

Carracedo, J. C., Geografía de Canarias, report, pp. 29-64, Insular Canaria, Tenerife, Spain, 1984.

Carracedo, J. C., The Canary Islands: An example of structural control on the growth of large oceanic island volcanoes, *J. Volcanol. Geotherm. Res., 60*, 225-241, 1994.

Carracedo, J. C., A simple model for the genesis of eruptive and large gravitational landslide hazards in the Canary Islands, *J. Geolog. Soc. London, 110*, 125-135, 1996.

Carracedo, J. C., and S. Day, Contrasting origin of the eastern and western Canary Islands, paper presented at XXI Meeting of the General Assembly, Int. Union Geod. and Geophys., Boulder, Colo., 1995.

Carracedo, J. C., S. J. Day, H. Guillou, E. Rodríguez Badiola, J. A. Canas, and F. J. Pérez Torrado, Geochronological, structural and morphological constraints in the genesis and evolution of an oceanic volcanic chain close to a passive continental margin: The Canary Islands, *Geol. Magazine*, in press, 1998.

Dainty, A.M., A scattering model to explain seismic Q observations in the lithosphere between 1 and 30 Hz, *Geophys. Res. Lett., 8*, 1126-1128, 1981.

Dañobeitia, J. J., J. P. Canales, and G. A. Dehghani, An estimation of the elastic thickness of the lithosphere in the Canary Archipelago using admittance function, *Geophys. Res. Lett., 21*, 2649-2652, 1994.

Fehler, M., M. Hoshiba, H. Sato, and K. Obara, Separation of scattering and intrinsic attenuation for the Kanto-Tokai region, Japan, using measurements of S-wave energy vs. hypocentral distance, *Geophys. J. Int., 108*, 787-800, 1992.

Frankel, A., and L. Wennerberg, Energy-flux model of the seismic coda: Separation of scattering and intrinsic attenuation, *Bull. Seismol. Soc. Am., 77*, 1223-1251, 1987.

Geisslinger, A., H. B. Hischleber, M. Schnaubelt, J. J. Dañobeitia, and J. Gallart, Mapping of volcanic apron and the upper crust between Gran Canaria and Tenerife (Canary Islands) with seismic reflection profiling, *GeoMar. Lett., 16*, 54-57, 1996.

Hayes, D. E., and P. D. Rabinowitz, Mesozoic magnetic lineations and the magnetic quiet zone off northwest Africa, *Earth Planet. Sci. Lett., 28*, 105-115, 1975.

Herrmann, R. B., Q estimates using the coda of local earthquakes, *Bull. Seismol. Soc. Am., 70*, 447-468, 1980.

Hoernle, K., and H. U. Schmincke, The role of partial melting in the 15-Ma geochemical evolution of Gran Canaria: A blob model for the Canarian hotspot, *J. Petrol., 34*, 599-626, 1993.

Holik, J. S., P. D. Rabinowitz, and J. A. Austin, Effects of the Canary hotspot volcanism on structure of oceanic crust off Morocco, *J. Geophys. Res., 96*, 12,039-12,067, 1991.

Hoshiba, M., Simulation of mutiple scattered coda wave excitation based on the energy conservation law, *Phys. Earth Planet. Inter., 67*, 123-136, 1991.

Hoshiba, M., Separation of scattering attenuation and intrinsic absorption in Japan using the multiple lapse time window analysis of full seismogram envelope, *J. Geophys. Res., 98*, 15,809-15,824, 1993.

Hoshiba, M., H. Sato, and M. Fehler, Numerical basis of the separation of scattering and intrinsic absorption from full seismogram envelope: A Monte-Carlo simulation of multiple isotropic scattering, *Pap. Meteorol. Geophys., 42*, 65-91, 1991.

Jin, A., K. Mayeda, D. Adams, and K. Aki, Separation of intrinsic and scattering attenuation in southern California using TERRAscope data, *J. Geophys. Res., 99*, 17,835-17,848, 1994.

Matsunami, K., Laboratory tests of excitation and attenuation of coda waves using 2-D models of scattering media, *Phys. Earth Planet. Inter., 67*, 104-114, 1991.

Mayeda, K., S. Koyanagi, M. Hoshiba, K. Aki, and Y. Zeng, A comparative study of scattering, intrinsic and coda Q^{-1} for Hawaii, Long Valley and Central California between 1.5 and 15.0 Hz, *J. Geophys. Res., 97*, 6643-6659, 1992.

McFarlane, D. J., and W. I. Ridley, An interpretation of gravity data for Tenerife, Canary Islands, *Earth Planet. Sci. Lett., 4*, 481-486, 1968.

Mézcua, J., J. Galán, J. J. Rueda, J. M. Marínez, and E.

Buforn, Sismotectónica de las Islas Canarias: estudio del terremoto del 9 de mayo de 1989 y su serie de réplicas, report, Inst. Geogr. Nac., Madrid, 1990.

Mézcua, J., J. J. Dañobeitia, A. Rivero, E. Banda, A. Checa, R. Parra, C. R. Ranero, J. J. Rueda, and A. Slootweg, Estudio geofísico de la cuenca oceánica del oeste del archipiélago canario, report, Inst. Geog. Nac., Madrid, 1991.

Pujades, L. G., J. A. Canas, J. J. Egozcue, M. A. Puigví, J. Pous, J. Gallart, X. Lana, and A. Casas, Coda *Q* distribution in the Iberian Peninsula, *Geophys. J. Int., 100*, 285-301, 1990.

Pujades, L. G., A. Ugalde, J. A. Canas, M. Navarro, F. J. Badal, and V. Corchete, Intrinsic and scattering attenuation from observed coda *Q* frequency dependence: Application to the Almeria Basin (southeastern Iberian peninsula), *Geophys. J. Int., 129*, 281-291, 1997.

Rautian, T. J., and V. I. Khalturin, The use of the coda for the determination of the earthquake source spectrum, *Bull. Seismol. Soc. Am., 68*, 923-948, 1978.

Roest, W. R., J. J. Dañobeitia, J. Verhoef, and B. J. Collete, Magnetic anomalies in the Canary Basin and the Mesozoic evolution of the central North Atlantic, *Mar. Geophys. Res., 14*, 1-24, 1992.

Sato, H., Multiple isotropic scattering model including P-S conversions for the seismogram envelope formation, *Geophys. J. Int., 117*, 487-494, 1994.

Shang, T., and L. S. Gao, Transportation theory of multiple scattering and its application to seismic coda waves of impulse source, *Sci. Sinica Ser. V, 31*, 1503-1514, 1988.

Verhoef, J., B. J. Collette, J. J. Dañobeitia, H. A. Roeser, and W. R. Roest, Magnetic anomalies off West-Africa (20-38°N), *Mar. Geophys. Res, 13*, 81-103, 1991.

Watkins, N.D., Paleomagnetism of the Canary Islands and Madeira, *Geophys. J. R. Astron. Soc., 32*, 1-19, 1974.

Watts, A. B., Crustal structure, gravity anomalies and flexure of the lithosphere in the vicinity of the Canary Islands, *Geophys. J. Int., 119*, 648-666, 1994.

Watts, A. B., and D. G. Masson, A giant landslide on the north flank of Tenerife, Canary Islands, *J. Geophys. Res., 100*, 24,487-24,498, 1995.

Wu, R. S., Multiple scattering and energy transfer of seismic waves: Separation of scattering effect from intrinsic attenuation, I, Theoretical modelling, *Geophys. J. R. Astron. Soc., 82*, 57-80, 1985.

Zeng, Y., F. Su, and K. Aki, Scattered wave energy propagation in a random isotropic scattering medium, I, Theory, *J. Geophys. Res., 96*, 607-619, 1991.

M. J. Blanco, Instituto Geográfico Nacional, Avenida Anaga 25, Planta 11, 38001 Santa Cruz de Tenerife, Spain.

J. A. Canas, Instituto Geográfico Nacional, General Ibáñez de Ibero 3, 28003 Madrid, Spain. (e-mail: canas@ign.es)

J. C. Carracedo and V. Soler, Estación Volcanológica de Canarias, Apartado de Correos 195, 38206 La Laguna, Spain. (e-mail: evc@iac.es)

L. G. Pujades, Enginyeria del Terreny i Cartogràfica, Universitat Politècnica de Catalunya, Gran Capità s/n D-2, 08034 Barcelona, Spain. (e-mail: pujades@etseccpb.upc.es)

A. Ugalde, Observatori de l'Ebre, Horta Alta 38, 43520 Roquetes, Spain. (e-mail: ugalde@etseccpb.upc.es)

(Received August 20, 1997; revised February 13, 1998; accepted March 2, 1998.)